D13-2004-47

V. L. Aksenov[1], K. N. Jernenkov[1], S. V. Kozhevnikov[1],
H. Lauter[2], V. Lauter-Pasyuk[1,2,3], Yu. V. Nikitenko[1],
A. V. Petrenko[1]

THE POLARIZED NEUTRON SPECTROMETER **REMUR** AT THE PULSED REACTOR **IBR-2**

[1]Frank Laboratory of Neutron Physics, JINR, 141980 Dubna,
Moscow Region, Russia
[2]Institut Laue Langevin, B.P. 156, F-38042, Grenoble, France
[3]Technische Universität München, D-85747 Garching, Germany

Аксенов В. Л. и др. Д13-2004-47

Спектрометр поляризованных нейтронов РЕМУР
на импульсном реакторе ИБР-2

Создан и введен в эксплуатацию новый спектрометр поляризованных нейтронов РЕМУР, предназначенный как для проведения исследований многослойных структур и поверхностей путем регистрации отражения поляризованных нейтронов, так и для изучения неоднородного состояния твердого тела с учетом диффузного рассеяния поляризованных нейтронов на малые углы. Спектрометр работает в интервале длин волн нейтронов 1÷10 Å и в рефлектометрическом режиме измерений позволяет осуществлять полный поляризационный анализ и позиционно-чувствительное детектирование нейтронов в телесном угле рассеяния $2{,}2\cdot10^{-4}$ рад. На спектрометре статистически обеспеченными являются рефлектометрические измерения в интервале изменения вектора рассеяния нейтронов $3\cdot10^{-3} \div 5\cdot10^{-1}$ Å^{-1}. В малоугловом режиме измерений спектрометр позволяет проводить исследование процессов рассеяния нейтронов без переворота спина в диапазоне телесного угла регистрации нейтронов детектором от $4\cdot10^{-3}$ до 10^{-1} рад в интервале значений вектора рассеяния от 0,006÷0,15 до 0,03÷0,7 Å^{-1} соответственно.

Работа выполнена в Лаборатории нейтронной физики им. И. М. Франка ОИЯИ.

Сообщение Объединенного института ядерных исследований. Дубна, 2004

Перевод авторов

Aksenov V. L. et al. D13-2004-47

The Polarized Neutron Spectrometer REMUR
at the Pulsed Reactor IBR-2

A new polarized neutron spectrometer REMUR has been constructed and commissioned. The spectrometer REMUR is dedicated to investigations of multilayers and surfaces by polarized neutron reflection and of the inhomogeneous state of solids by diffuse small-angle polarized neutron scattering. The spectrometer operates in the neutron wavelength interval 1÷10 Å. In the reflectometry mode it allows one to complete polarization analysis and neutron position-sensitive detection within the solid angle of scattering $2{.}2\cdot10^{-4}$ rad. The spectrometer ensures good statistics of the reflectometric data in the scattering wave vector interval $3\cdot10^{-3} \div 5\cdot10^{-1}$ Å^{-1}. In the small-angle scattering mode the spectrometer allows the investigation of neutron scattering processes without spin-flip over the detector's neutron registration solid angle interval from $4\cdot10^{-3}$ to 10^{-1} rad and the scattering wave vector interval from 0.006÷0.15 to 0.03÷0.7 Å^{-1}, respectively.

The investigation has been performed at the Frank Laboratory of Neutron Physics, JINR.

Communication of the Joint Institute for Nuclear Research. Dubna, 2004

INTRODUCTION

Originally, polarized neutrons were used to study the structure of the inhomogeneous magnetic state of ferromagnetics by measuring the polarization of the polarized neutron beam transmitted through the sample (neutron depolarization method) [1–3]. At present, the field of polarized neutron applications has essentially widened. Today, it includes, for example, studies of the structure of magnetics by diffuse neutron scattering [4], investigations of magnetic excitations in ferromagnetics by measuring the angular distribution of the scattered polarized neutron [5], studies of low-frequency excitations in solids by the neutron spin-echo method [6] and, finally, studies of the layered nanostructure by neutron reflection (neutron reflectometry method [7]). Neutron reflectometry as a method for the investigation of solid body surfaces started to be intensely developed comparatively recently, in the 1980s. One of the first polarized neutron reflectometers in the world is the polarized neutron spectrometer SPN put into operation at the IBR-2 reactor in 1984. An original element in SPN is the Korneev spin-flipper with a stretched working area in the vertical direction [8, 9]. The first experiments with SPN were made in the depolarization mode. Then it operated as a neutron reflectometer for a long time [10]. Today, rapid advances in nanotechnology require the creation of complicate magnetically noncollinear periodic structures and bilayers with perfect interfaces, plane-structured nanostructures, structures with zigzag-like interfaces, etc. [11]. To serve the purpose, in various neutron research centers about forty neutron reflectometers have been built and the polarized neutron reflectometry method is being intensely developed. The development goes in the following directions: increasing of the information density of measurements, raising of the polarization efficiency of the spectrometer, extending of the measurement range and increasing of the momentum transfer measurement resolution, increasing of the luminosity of measurements, of the measuring sensitivity of a specified parameter (e.g., an absolute value of the magnetization vector, rotation angle of the magnetization vector, layer thickness, etc.), increasing of the scattered neutron registration solid angle, and reducing of the neutron count intensity background. Nanoroughnesses in the vicinity of the interface, magnetic or nuclear inhomogeneities in some layers affect one or another interaction or microproperty of the structure. Therefore, of importance is the registration of the diffuse scattering of polarized neutrons by the structure. In this connection, it should be noted

that the neutron reflectometry method is compatible, in terms of its technical realization, with the method of diffuse neutron scattering on inhomogeneities in the medium. In fact, the experimental basis of the neutron reflectometry method is that it is necessary to measure neutron reflection in the vicinity of the critical wave vector transfer $k_c = 4\pi \sin\theta_c/\lambda$, where λ is the neutron wavelength, θ_c is the critical neutron glancing angle. The value of k_c depends on the density of nuclei and the neutron scattering amplitude on the nucleus and is of the order $2 \cdot 10^{-2}$ Å^{-1}. For thermal neutrons with the wavelength $\lambda = 1.8$ Å it corresponds to the scattering angle $\theta_{\mathrm{scat},r} = 2\theta_c \approx 6 \cdot 10^{-3}$ rad. At the same time, the experimental basis of the diffuse neutron scattering method is to conduct measurements in the vicinity of the wave vector transfer $q = 2\pi \sin(\theta_{\mathrm{scat},d})/\lambda = 2\pi/d$, where d is the linear dimension of the inhomogeneity in the medium (correlation length). From the equation for q it follows that if ≈ 300 Å, the scattering angle is $\theta_{\mathrm{scat},d} \approx 5.9 \cdot 10^{-3}$, which is close to the critical scattering angle $\theta_{\mathrm{scat},r}$ in the reflectometry method. So, the correspondence between the angular characteristics of the two types of neutron scattering, the necessity to know the structure and the distortions it has at interfaces as well as the level of substance homogeneity in the structure's layers point to the fact that it is important to envisage in the polarized neutron spectrometer the registration of specular and diffuse reflection from interfaces or surfaces as well as the registration of small angle neutron scattering on inhomogeneities in the medium volume.

1. THE FUNCTIONAL SCHEME OF THE SPECTROMETER

In the polarized neutron spectrometer REMUR there is realized:

1. Mode to measure the reflection of polarized neutrons and their transmission through a layered structure (reflectometric mode), and the mode to measure diffuse small-angle neutron scattering (small-angle mode).

2. Complete polarization analysis of the reflected and the scattered neutron beam [12] that allows the investigation of processes with/without a change in the neutron spin state.

3. Polarization analysis of the neutron beam with respect to the local field in the investigated sample based on the effect of spatial splitting of the neutron beam that occurs if there exists a nonzero probability of neutron transition between spin states.

4. Position-sensitive detection of neutrons with the angular resolution in the horizontal plane ± 0.17 mrad.

5. Shifting of the polarization efficiency of the reflectometric mode in the neutron wavelength interval $1.5 \div 5$ Å accomplished by changing the glancing angle of the neutron beam falling on the supermirror of the neutron polarizer.

6. Automated switching over of the state of the spectrometer during its operation in a specified mode, automated acquisition of the spectrometric data, control of the state of individual blocks of the spectrometer.

7. Visualization and express-analysis of the spectrometric data.

Figure 1 shows the functional scheme of the spectrometer. The fast neutrons formed in the active zone (AZ) of the reactor get thermolized in the water moderator WM situated around the AZ. The moderator thickness is 5 cm, which sets the time of fast neutron moderation and the thermal neutron pulse duration at 320 μs [13]. The moment of thermal neutron emission from the moderator is further used as a reference point to determine the time of neutron flight from moderator to neutron detector. The time of flight, in turn, determines the neutron wavelength, which is the essence of the time-of-flight method at the pulsed neutron source. The thermal neutron beam emitted from the moderator is shaped using the double-disc neutron chopper DCh (the chopper-to-moderator distance is $L_1 = 4.5$ m). The neutron chopper transmits the main thermal neutron pulse and shuts off four satellite pulses of thermal neutrons arising in a period of time multiple of 40 μs after the main pulse was generated. The satellite pulses arise due to that the auxiliary neutron reflector passes by the active zone. Leaving the chopper the neutron beam enters the collimator C1 situated in the wall of the reactor biological shielding (the diameter of the round inlet in the collimator is 200 mm, the collimator-to-moderator distance is $L_2 = 9$ m), goes along the conic convergent neutron guide NG and enters the second collimator C2 at the exit of the neutron guide (the cross section of the inlet in the collimator is 20×160 mm^2, the distance from the moderator is $L_3 = 20$ m). Along the 4.5 m path behind the second collimator the systems formed the polarized neutron beam for the reflectometric and small-angle modes of the spectrometer are installed in the direction of the beam and parallel to each other. Each of them consists of two units fixed, respectively, to two movable platforms PL1 ($L_4 = 20.5$ m) and PL2 ($L_5 = 24.5$ m) shared by the systems. The platforms stretching 1200 mm in the direction of the neutron beam have drives at the ends to displace them across the beam. The drives are used to adjust the units with respect to the neutron beam.

The polarized neutron beam formation system for the reflectometric mode includes the collimator CR1, neutron polarizer PR and the collimator CR2. The 1200 mm long collimator CR1 is fixed to the first platform and has the inlet 10×80 mm^2. The polarizer PR fixed to the second platform is a supermirror on a glass substrate measuring $28 \times 100 \times 800$ mm^3. The collimator CR2 is 400 mm long and its inlet has the exit cross section 2×80 mm^2. An optimal situation of the collimator CR2 that would provide for the transmission of the neutron beam reflected from the polarizer and a low fast neutron background level is achieved by rotating the collimator about the rotation axis coinciding with the polarizer exit. At the exit of the collimator a neutron beam with the cross section 2×80 mm^2 is formed.

The polarized neutron beam formation system for the small-angle mode consists of the polarizer PM and the collimator CM fixed to the first and second platforms, respectively. The polarizer is a stack of 300 mm long straight supermirrors 1 mm apart. The inlet in the polarizer has the cross section 38 (horizont.) $\times$ 42 (vert.) mm^2. At the exit of the polarizer a neutron beam with the cross section 20×42 mm^2 is formed. The collimator CM is 1200 mm long and has an inlet with the cross section 40×40 mm^2.

On its way to the sample the formed polarized neutron beam also goes through the cadmium diaphragm D1 ($L_6 = 25$ m), exit collimator C3 ($L_7 = 26$ m), spin-flipper SF1 and the second diaphragm D2 ($L_7 = 28.5$ m). The cross section of the inlet in the diaphragm is adjusted within the limits $(0 \div 50) \times (0 \div 160)$ mm^2 by remote control. The cross section of the inlet in the collimator C3 is 100×200 mm^2. The gradient radiofrequency (RF) spin-flipper is a 160 mm diameter by 300 mm length solenoid surrounded with curved coils of special design which changes to the opposite the neutron beam polarization. The alternating magnetic field of 10 Oe at 75 Hz is directed along the solenoid axis parallel to the neutron beam and the permanent magnetic field generated by the coils is perpendicular to the direction of the neutron beam, and it varies from 40 to 10 Oe along the beam direction.

The sample position is at $L_8 = 29$ m behind the moderator. The sample is in a special holder to the entrance and exit of which diaphragms made of 1 mm sheet cadmium can be fixed. In the reflectometric mode the neutrons reflected from the sample go through the second spin-flipper SF2 (SF2 is analogous to SF1), the focused (fan-shaped) beam polarization analyzer APF ($L_9 = 33.4$ m) [14] and are registered with the position-sensitive detector PSD ($L_{10} = 33.7$ m) [15]. The described equipment can be also used for small-angle investigations in the slit geometry as is shown in [15].

In the small-angle mode neutrons are registered with the multicounter (32-counter) neutron detector (MCD) located at $1.5 \div 7.5$ m from the sample.

2. THE EQUIPMENT OF THE SPECTROMETER

2.1. Polarizers and Polarization Analyzer. The polarizers and polarization analyzer are made from supermirror with the critical angle of thermal neutron reflection $\theta_c(\lambda = 1.8\ \text{Å}) = 6.3$ mrad which is 2 times larger than that from the surface made from natural nickel [16]. Since the neutron beam glancing angle in the polarizer (polarization analyzer) θ is fixed, to the critical angle $\theta_c(\lambda = 1.8\ \text{Å})$ there corresponds the critical wavelength $\lambda_c\ (\text{Å}) = 1.8\theta/\theta_c(\lambda = 1.8\ \text{Å})$. As is known, the principle of operation of the supermirror polarizer (polarization analyzer) consists in that neutrons whose spin projection lies in the direction of the magnetic field (neutrons in «+» spin state) are reflected from the magnetic

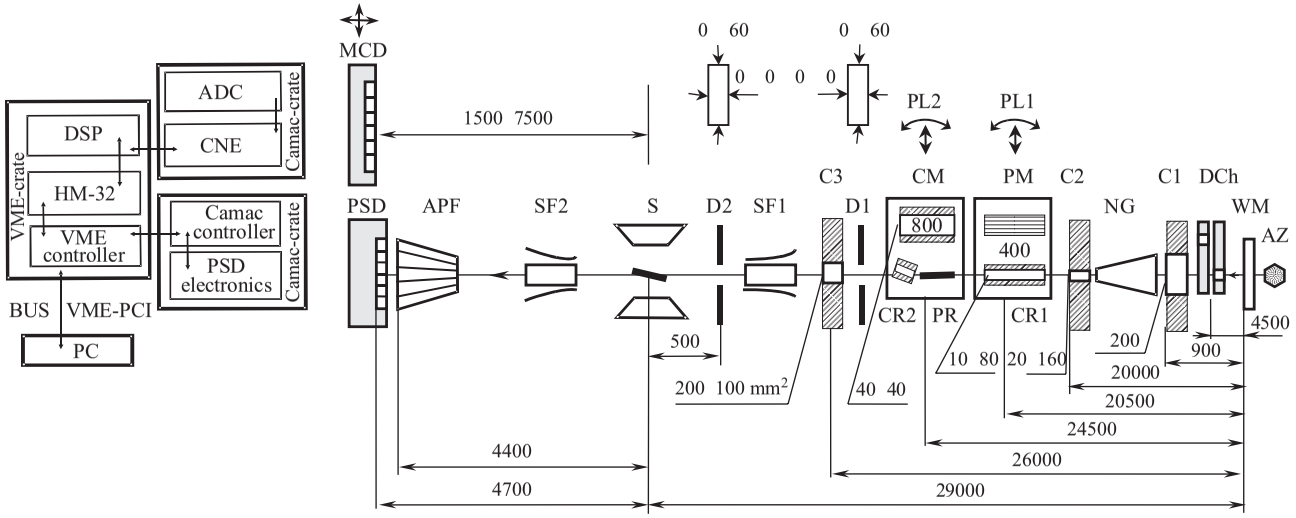

Fig. 1. The functional scheme of the REMUR spectrometer: AZ — active zone of the reactor; WM — water moderator; DCh — double disk chopper; C1, C2, C3 – collimators; NG — conic neutron guide; PL1, PL2 — controlled platforms No. 1 and No. 2; CR1, CR2 — reflectometric collimators; PR –reflectometric polarizer; PM — small-angle polarizer; CM — small-angle collimator; D1, D2 — controlled diaphragms; SF1, SF2 — spin-flippers; S — sample; APF — focused polarization analyzer; PSD — position-sensitive detector; MCD — small-angle multi-counter detector

supermirror layer and neutrons with the spin projection in the opposite to the magnetic field direction (neutrons in «-» spin state) are transmitted through the layer and get absorbed in the next layer that has a larger neutron capture cross section. The ratio of the reflected neutrons in the «+» to «-» spin state $r = j^+/j^-$ determines the polarization efficiency of the polarizer (polarization analyzer) $P = (r-1)/(r+1)$. The polarization efficiency P is close to unity (at the same time, $r \gg 1$) if $\lambda \geqslant \lambda_c$ for which the reflectivity of neutrons in the «+» spin state is $R^+ \approx 1$ and for the reflectivity there holds the condition $R^+ \gg R^-$.

The polarizer in the reflectometric mode is a glass plate measuring $H \times D \times L = 100 \times 28 \times 800$ mm^3 whose $H \times L$ surface is covered with a supermirror layer. The side L is along the neutron beam and the sides H and D are directed across the beam, H in the vertical and D in the horizontal direction. The plate thickness $D = 28$ mm is chosen to provide for sufficient flatness of the plate from the viewpoint of ensuring a not large angular width of the reflected neutron beam. The width of the polarized neutron beam d (in the direction perpendicular to the mirror plane) that in certain conditions determines largely the angular resolution of the spectrometer is related to the neutron beam glancing angle θ and the supermirror polarizer length l as $d = l\theta$. The neutron beam glancing angle at the polarizer can be adjusted within the limits $3 \cdot 10^{-3} \div 10^{-2}$ rad by rotating the supermirror, which gives $d = 0.24 \div 0.8$ mm. At the same time, the critical wavelength changes within the limits $0.86 \div 2.84$ Å, respectively.

To execute the small-angle mode, there are envisaged two polarizers: a stack of straight mirrors (SSM) and a stack of curved mirrors (SCM). A stack of mirrors is used because of the necessity to obtain, on a limited distance along the beam, a polarized neutron beam with a large cross section. Due to the possibility to have a not large neutron glancing angle the polarizer SSM is characterized by not large value of λ_c, which is important in the work with a «warm» neutron source. The average glancing angle in SSM is $\theta_{\rm av} = \Delta d/l$, where Δd is the spacing between mirrors equal to 1 mm in the discussed SSM. If the mirror length $l = 300$ mm, $\theta_{\rm av} = 3.3 \cdot 10^{-3}$ rad, which gives the critical length $\lambda_c = 0.94$ Å. The disadvantage of SSM is that part of neutrons may go through the polarizer without being reflected from the mirror if no special measures are taken. As a result, the polarization efficiency of the polarizer reduces. To avoid the efficiency reduction, the condition $d < 2L_{\rm ps} \cdot \theta_{\rm av}$, where $L_{\rm ps}$ is the polarizer-to-sample position distance, must be met. It is chosen that in the spectrometer $L_{\rm ps} = 9$ m, which gives the maximum beam width $d_{\max} = 59.4$ mm. The value of $d_{\max}$ reduces, however, to 40 mm due to beam divergence and a finite size of the sample.

On the other hand, the advantage of the polarizer SCM is the absence of direct sight through it. At the exit of such a polarizer there will be only the neutrons reflected from the polarizer's mirror. As a result, the maximum neutron beam width equals the width of the inlet in the polarizer. For SCM, however, λ_c appears

to be larger than for SSM and is determined by a number of parameters [17]: $\lambda_c = 4a/l_d\sigma$, where $l_d = 2(2a\rho)^{1/2}$ is the length of direct line of sight, a is the channel width, ρ is the radius of curvature, $\sigma = (Nb/2\pi)^{1/2}$, N is the density of nuclei in the matter, b is the coherent scattering amplitude that is a sum of the nuclear and magnetic amplitudes. For SCM in the spectrometer REMUR, $l_d = 500$ mm, $a = 0.6$ mm and $\sigma = 3.5 \cdot 10^{-3}$ A^{-1}, which gives $\lambda_c \approx 1.4$ Å.

The analyzer in the spectrometer REMUR is unique [14]. Somewhat analogous is the analyzing system of mirrors in the small-angle scattering spectrometer in Petersburg Institute of Nuclear Physics (PNPI), RAS in Gatchina [18]. In the reflectometric experiment with prevailing specular reflection, of special importance, however, is the positional relationship between the investigated sample and analyzer mirrors. While in the conventional analyzer the mirrors plane is oriented to be perpendicular to the sample or parallel to the scattering plane, in the REMUR polarization analyzer the planes of the polarizer mirrors and of the sample are parallel to each other. At the same time, each mirror in the analyzer is oriented so that it formed a certain, equal for all of them, angle with a straight line drawn from one point, the focus of the analyzer. The stack of mirrors looks like a fan and this is why the focused analyzer is called a fan-like analyzer. The investigated sample is placed in the focus of the analyzer. The focal distance of the analyzer is 4400 mm, the distance between 0.3 mm thickness mirrors is 0.93 mm at the entrance and 1 mm at the exit and the neutron beam glancing angle on the mirror (the inclination angle of the mirror plane with respect to the radius vector drawn from the focus) is 4.5 mrad. The mean square uncertainty of the neutron beam glancing angle on one mirror in the analyzer is 0.09 mrad, which is 2 times smaller than an analogous value for the detector and it does not virtually lead to a decrease in the neutron detection resolution. At the same time, the relative mean square deviation of the glancing angle on the mirror is 2 % and the mean square dispersion over mirrors of the polarization efficiency does not exceed 0.5 %. It is obvious that to have these very parameters of polarization efficiency in the presence of the sample, the neutron beam width on the sample (sample effective thickness) must not be larger than half the discreteness step in the analyzer $\Delta d/2 = 0.65$ mm. At the same time, the size of the sample in the direction of the beam must be not larger than 90 mm and the precision of sample positioning in the direction across the beam must be not worse than 0.2 mm. As a rule, such requirements are satisfied in the reflectometric mode. An important advantage of analyzers of the type is their high luminosity. It is due to the fact that if the analyzer mirrors and the sample have a vertical orientation, as it is the case in the fan-like analyzer, they appear to be matched with respect to divergence in the horizontal and vertical planes. Let us make assessments of the luminosity gain in the REMUR analyzer in comparison with the conventional analyzer. For the REMUR analyzer we have the relationship $S_f = S_a\Omega_s = S_aS_s/L_{sa}^2$ for the product of the analyzer inlet cross-section area

S_a and the solid angle of sample acceptance Ω_s, where $S_s = h_s d_s$ is the sample cross-section area, $S_a = h_a d_a$ is the analyzer cross-section area, h_s and h_a are the sizes of the sample and the analyzer, respectively, in the direction of the sample plane orientation, $d_s = l_s \sin(\theta)$ and d_a are the effective size of the sample and

Table 1. The parameters of the polarizers and analyzers of the REMUR spectrometer

Reflectometric polarizer: one mirror	
Substrate dimensions	$28 \times 100 \times 800$ mm^3
Polarized neutron beam cross section	$0.24 \div 0.8$ mm
Beam glancing angle	$1 \div 3.3$ mrad
Critical wavelength	$0.86 \div 2.84$ Å
Small-angle polarizer: stack of straight mirrors	
Number of mirrors:	32
Glass substrate thickness	0.2 mm
Spacing between mirrors	1 mm
Mirror length	300 mm
Coating	on two sides
Polarized neutron beam cross section	20×42 mm^2
Inlet cross section (vent. $\times$ horiz.)	42×38 mm^2
Critical wavelength	0.94 Å
Small-angle polarizer: stack of curved mirrors	
Number of mirrors	45
Substrate thickness	0.3 mm
Spacing between mirrors	0.6 mm
Mirror length	$2 \times 260 = 520$ mm
Coating on two sides	50(FeCo/TiZr)
Inlet cross section (vert. $\times$ horiz.):	40×40.2 mm^2
Radius of curvature	50 m
Critical wavelength $\lambda_{\mathrm{crit.}}$	1.4 Å
Reflectometric analyzer: stack of focused mirrors	
Number of mirrors	94
Substrate dimensions	$250 \times 60 \times 0.3$ mm^3
Mirror inclination angle with respect to radius vector drawn from focus	4.5 mrad
Channel cross section input	0.93×40 mm^2
output	1.0×40 mm^2
Beam capture angle in horizontal plane	27.3 mrad
Focal distance	4400 mm
Inlet cross section (vert. $\times$ horiz.)	40×120 mm^2
Transmission «geometric»	0.66
Coating on two sides	FeCoV/TiZr
Critical wavelength	1.3 Å

the size of the analyzer mirror, respectively, in the direction perpendicular to the sample plane, L_{sa} is the sample-to-analyzer distance.

For a conventional analyzer we have $S_n = S_s \delta\theta_a (h_a/L_{sa})$, where $\delta\theta_a$ is the mean square value of the glancing angle at which the mirror of the analyzer works effectively. The luminosity gain is determined by the factor $\beta = S_f/S_n = d_a/(\delta\theta_a L_{sa})$. Let $\delta\theta_a$ be $\Delta d_a/4l_a$, where l_a is the length of the mirror and Δd_a is the distance between the mirrors in the analyzer. Then $\beta = 4d_a l_a/(\Delta d_a L_{sa})$. If $d_a = 38$ mm, $l_a = 300$ mm, $\Delta d_a = 1$ mm, $L_{sa} = 4400$ mm in the analyzer, $\beta \approx 10$. So, the gain increases with increasing d_a and decreasing L_{sa}, and $l_a/\Delta d_a$ is a constant that characterizes the mirror quality. Table 1 summarizes the parameters of three different polarizers and the polarization analyzer of the REMUR spectrometer.

Figure 2 shows the reflectivity for «+» spin neutrons (Fig. 2, *a*, *c*) and the polarization efficiency of mirrors the fan-like analyzer and the SCM polarizer

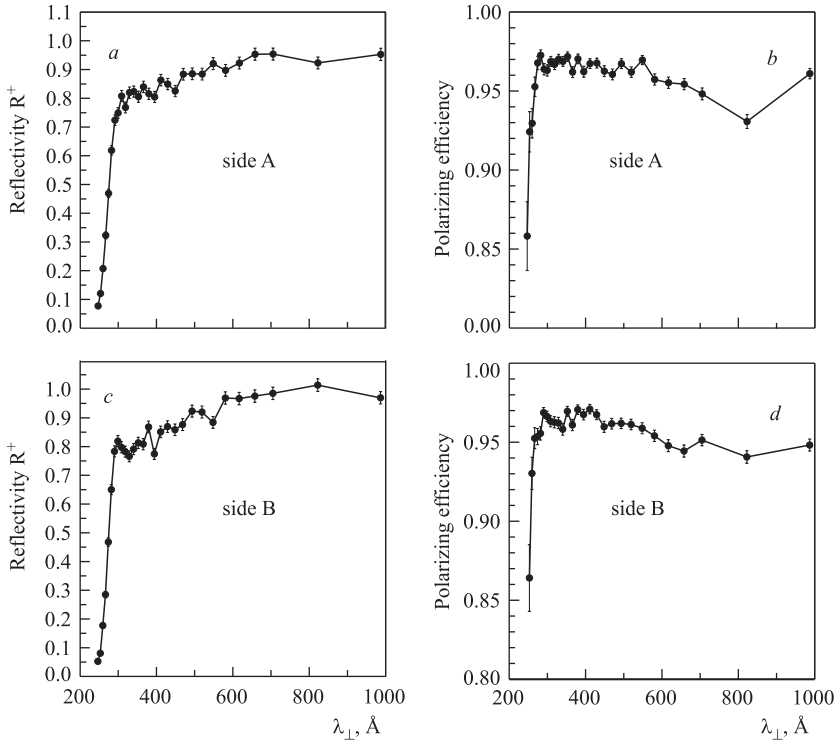

Fig. 2. The reflectivity of neutrons with the plus spin component from (*a*, *c*) and the polarization efficiency of the supermirror (*b*, *d*) as a function of the neutron wavelength normal to the mirror surface (the neutron wavelength is 1.435 Å). *a*, *b*) — one side of the mirror, *c*, *d*) — the other side of the mirror

(Fig. 2, *b*, *d*) are made from. Figure 2, *a*, *b* presents the data for one side and Fig. 2, *c*, *d* — for the other side of the mirror. The measurements were conducted for the neutron wavelength 1.435 Å. In Fig. 2, the X-axis shows the parameter λ/θ, the «perpendicular» wavelength. First of all it is seen that the characteristics of the mirrors are the same for their two sides. Second, it is seen from Fig. 2, *a*, *c* that the critical value of the perpendicular wavelength is $\lambda_\perp = 300$ Å, which gives $\sigma = 1/\lambda_\perp = 3.3 \cdot 10^{-3}$. From Fig. 2, *b*, *d* it is seen that starting from $\lambda_\perp = 500$ Å the polarization efficiency somewhat drops. It is due to the corresponding growth of the neutron reflection coefficient for the «-» spin component (which is obvious if one considers the dependence $R^+(\lambda)$). Figure 3 illustrates the wavelength dependence of the polarization efficiency of the reflectometric polarizer (curve *1*), fan-like analyzer (curve *2*), curved analyzer for the small-angle mode (curve *3*), and the straight polarizer for the small-angle mode (curve *4*). For the sake of comparison there is also shown an analogous curve for the polarization efficiency of the polarizer in the SPN spectrometer (curve *5*) [10]. It is seen that in the wavelength interval $\lambda > 2$ Å the polarization efficiency curves of the polarizers and the polarization analyzer in REMUR go higher above the polarization efficiency curve for the SPN polarizer.

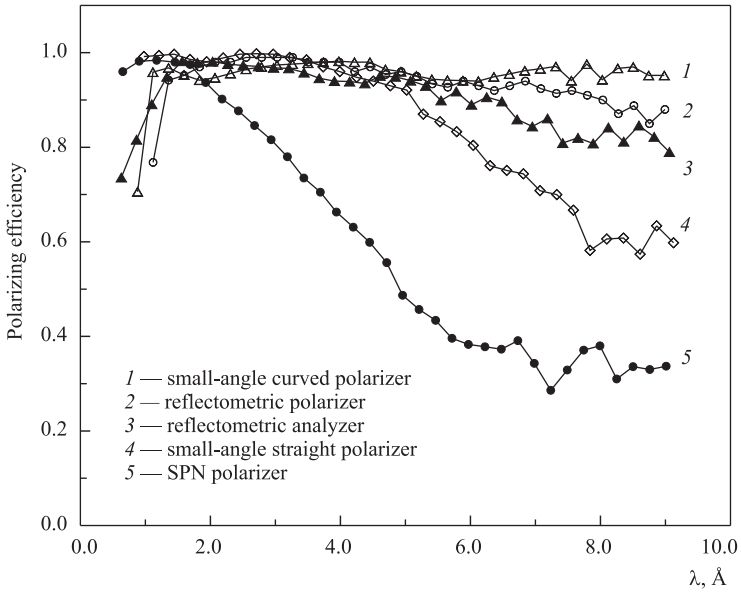

Fig. 3. The wavelength dependence of the polarization efficiency: *1* — small-angle curved polarizer; *2* — reflectometric polarizer (the glancing angle is 4.6 mrad); *3* — focused polarization analyzer (the glancing angle is 4.5 mrad); *4* — small-angle straight polarizer (the glancing angle is 4.6 mrad); *5* — SPN spectrometer polarizer

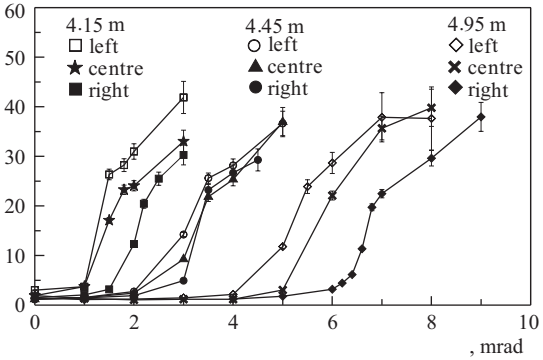

Fig. 4. The polarization ratio η over the wavelength interval $1.4 \div 10$ Å as a function of the analyzer rotation angle α for the diaphragm-to-analyzer distances 4.15, 4.45 or 4.95 m

Figure 4 shows the polarization ratio η between spin-flipper off/on neutron counts over the wavelength interval $1.4 \div 10$ Å as a function of the analyzer rotation angle α and the situation of the neutron beam on the analyzer on the left of the center (if viewed in the direction of the neutron beam), in the center or on the right of the center. The diaphragm at sample position has a width of 0.5 mm and the neutron beam width on the detector is 14 mm. The diaphragm-to-analyzer distances are 4.15, 4.45 or 4.95 m. It is seen that for the distance 4.45 m the curves corresponding to the different situations of the neutron beam coincide. This is an indication of that the diaphragm is in the focus of the analyzer if the distance between them is 4.45 m.

2.2. Spin-Flippers. In the spectrometer REMUR there is employed a gradient RF spin-flipper [19–22] whose permanent and alternating magnetic fields vary sinusoidally as a function of the coordinate z along the neutron beam direction. The permanent magnetic field varies as $H_0(z) = H_0(z_0) + A\cos(\pi z/L_{\rm SF})$ and the amplitude of the alternating magnetic field is described by the equation $H_{\rm rf}(z) = 2A\sin(\pi z/L_{\rm SF})$, where $L_{\rm SF}$ is the spin-flipper length, $z_0 = L_{\rm SF}/2$ is the coordinate of the spin-flipper center, $A = H(0) - H(z_0)$ is the modulation amplitude. The alternating magnetic field frequency equals the Larmor precession frequency of neutrons ω_L in the magnetic field $H(z_0)$ in the center of the spin-flipper. The probability of neutron spin flip due to the described spin-flipper is [23]

$$f = \frac{k^2 + \cos^2((\pi/2)\sqrt{1+k^2})}{k^2+1}. \qquad (1)$$

To derive Eq. (1), it is assumed that the adiabatic ability parameter $k = \gamma H_e/\Omega$ is a constant. Here $H_e = [(H(z) - H(z_0))^2 + (H_{\rm rf}/2)^2]^{1/2}$ is the effective magnetic

field, $\Omega = v(H_{\rm rf}/2)[d(H(z) - H(z_0))/dz]/H_e^2$, v is the neutron velocity, γ is the neutron gyromagnetic ratio. Figure 5 illustrates the dependence of the spin-flip probability on the parameter of adiabatic ability. It can be seen that some specified minimum $f_{\rm min}$ is achieved at a minimal $k_{\rm min}$ corresponding to the minimal neutron wavelength $\lambda_{\rm min}$. As further the wavelength increases to infinity, $f(\lambda)$ grows and tends to unity. So, the working wavelength interval of a spin-flipper with $f_{\rm min} < f < 1$ is $\lambda \geqslant \lambda_{\rm min}$. Using $H(z)$ and $H_{\rm rf}(z)$ in the explicit form we obtain

$$k = \gamma A L_{\rm SF}/[\pi v \sin^2(\pi z/L_{\rm SF})]. \qquad (2)$$

From Eq. (2) it is seen that k is a function of the coordinate z and is inversely proportional to the neutron velocity. As a result, for a minimal k we obtain $k_{\rm min} = \gamma A L_{\rm SF}/(\pi v_{\rm max})$ and for an averaged over coordinates k we have $k_{\rm av} = 2k_{\rm min} > k_{\rm min}$. The equation $k_{\rm av} = 2\gamma A L_{\rm SF}/(\pi v)$ can be used for the estimation of the spin-flipper parameters. Let $f_{\rm min}(\lambda_{\rm min} = 1\ \text{Å}) \geqslant 0.99$ correspond to $k_{\rm av}(\lambda_{\rm min} = 1\ \text{Å}) = 10$. For the specified length $L_{\rm SF} = 500$ mm we obtain $A = 7.5$ Oe. The calculation technique of the gradient RF spin-flipper is described in detail in [20]. It is chosen that in the REMUR spin-flippers $H(z_0) = 26$ Oe which corresponds to the frequency 76 kHz of the RF magnetic field. The spin-flipper is controlled manually or automatically by means of a special flipper drive (FD). Direct current from a power supply is supplied to FD that generates a 76 kHz signal to a RF coil. The alternating magnetic field amplitude is regulated by direct current from the power supply. The permanent magnetic field changes in dependence on the current in the leading coils. The tuning process of the gradient RF spin-flipper is described in more detail in [22]. From Fig. 6 it is seen that a real distribution of magnetic fields over the length of the gradient spin-flipper is

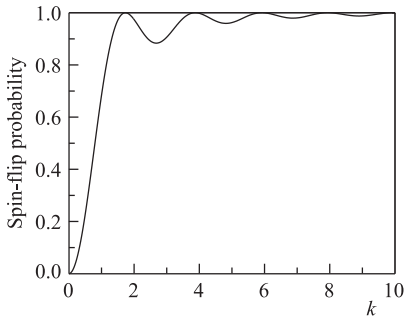

Fig. 5. The neutron spin-flip probability in a system of skew harmonic magnetic fields as a function of the adiabatic ability parameter

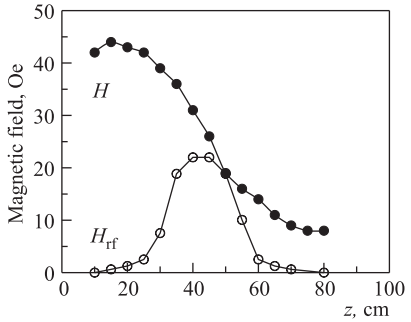

Fig. 6. The real distribution of magnetic fields over the length of the RF gradient spin-flipper

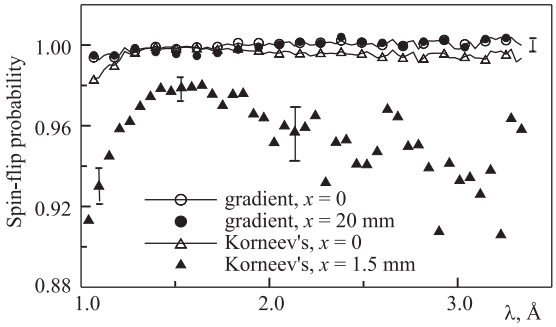

Fig. 7. The wavelength dependence of spin-flip probability in dependence on the situation of the beam x with respect to the center of the spin-flipper: ○ — gradient spin-flipper, $x = 0$; ● — gradient spin-flipper, $x = 20$ mm; △ — Korneev spin-flipper, $x = 0$; ▲ — Korneev spin-flipper, $x = 1.5$ mm

close to sinusoidal. The guide magnetic field outside the spin-flipper region is about 10 Oe.

Among the advantages of the gradient RF spin-flipper are:

1) A noncollimated neutron beam (divergence up to 0.1 rad) with a large cross section (~ 100 cm^2);

2) No strong requirements for the stability and homogeneity of the magnetic fields or for the stability of the alternating magnetic field frequency;

3) The absence of substances on the way of the neutron beam.

Figure 7 depicts the wavelength dependence of the spin-flip probability for the gradient RF and Korneev spin-flippers measured with a 1.5 mm wide by 30 mm high neutron beam [8, 9]. The curves *1* and *2* are of the gradient RF spin-flipper with the beam situation in the center and at 200 mm off the center of the spin-flipper. The curves *3* and *4* are of the Korneev spin-flipper with the beam situation in the center and at 1.5 mm of the center of the flipper, respectively. It is clearly seen that the spin-flip probability in the Korneev spin-flipper changes significantly at the smallest displacement of the beam. And vice versa, it does

Table 2. The parameters of the gradient RF spin-flippers

	First spin-flipper	Second spin-flipper
Vacuum tube inner diameter, mm	150	100
Dimension: length × width × height, mm^3	800 × 360 × 520	800 × 320 × 530
1) Permanent magnetic field coil:		
1 mm diameter copper wire		
Coil resistance, Ohm	32.3	23.4
Coil current, A	1.8	2.2
2) RF coil:		
Coil length along the beam, mm	300	300
Alternating magnetic field frequency, kHz	76.4	73.4
Direct current from power supply, A	1.5	1.3
Power supply consumed voltage, V	22	14

not practically change in the gradient spin-flipper at a sizable displacement of the neutron beam situation. Table 2 summarizes the parameters of the spin-flippers included in the REMUR layout.

2.3. Neutron Detectors

2.3.1. The Detector for the Reflectometric Mode. In the reflectometric mode of the REMUR spectrometer neutrons are registered with a gas-filled one-dimensional position sensitive detector (PSD) [15]. The employment of PSD instead of the gas-filled neutron counter used earlier has made it possible to simplify considerably the process of sample adjustment, reduce the statistics acquisition time several times when the sample causing diffuse neutron scattering is studied, made it possible to perform the monitoring of the intensity of neutrons by measuring the direct and the scattered beams simultaneously, to conduct, in the absence of diffuse scattering, simultaneous measurements of the intensity of specular beams and the background.

PSD is a proportional multiwire cell in a hermetic duraluminium box with a 120×40 mm^2 cross-section inlet. The inside dimension of the box is $200 \times 100 \times 48$ mm^3. The registration of neutrons is based on the reaction of neutron capture in ^{3}He nuclei and the emission of secondary fission products, protons and tritium nuclei: $^3\mathrm{He}(n,p)^3\mathrm{H} + 764$ keV. The gas layer thickness is 24 mm at a ^{3}He pressure of 3.4 atm. To raise the spatial resolution, propane with a partial pressure of 2 atm, is added to the volume of the gas in the detector. The spatial resolution of the detector is $1.5 \div 2.5$ mm (FWHM). The highest resolution, on the order of 1.5 mm, is achieved in the center of the detector. The width of the position channel of the detector is 0.69 mm and the number of position channels is 256. The duration of the time channel is 128 μs and their number is 2048. The dead time of the detector is 37 ns. The parameters of the detector are summarized in Table 3.

Table 3. The PSD parameters

Gas mixture	^{3}He (3.4 atm) + C_3H_8 (2 atm)
Sensitive volume dimension	$120 \times 40 \times 24$ mm^3
Inlet window dimension	120×40 mm^2
Inlet window material	Al (alloy D16T)
Spatial resolution (FWHM)	in the center — 1.5 mm at edges — 2.5 mm
Registration efficiency for $\lambda = 2$ Å	70%

To determine the PSD neutron registration efficiency, in addition to PSD there was used a monodetector (helium counter CHM-17, time channel width 64 μs, number of channels 2048) placed immediately before the PSD. Three count intensities were measured: J_p — the PSD count intensity without the

monodetector, J_m — the count intensity of the monodetector, and J_{pm} — the PSD count intensity with the monodetector. The following relationships can be written for them:

$$J_m = J_0 A_m \varepsilon_m, \quad J_p = J_0 A_p \varepsilon_p, \quad J_{pm} = J_0 A_p \varepsilon_p A_m^2 (1 - \varepsilon_m),$$

where J_0 is the neutron beam intensity before the detector; $A_m = \exp(-b_m \lambda)$ is the neutron transmission coefficient of the monodetector wall; $A_p = \exp(-b_p \lambda)$ is the neutron transmission coefficient of the PSD inlet window; $\varepsilon_m = 1 - \exp(-c_m \lambda)$ and ε_p are the neutron registration efficiency of the monodetector and PSD, respectively; λ is the neutron wavelength. To write the monodetector neutron registration efficiency in an explicit form, it is assumed that the registration efficiency is only determined by neutron absorption in the gas (the read-out efficiency of the electronics is considered to be equal to unity). For ε_m, ε_p, and J_0 we have the following relationships:

$$\varepsilon_m = 1 - \frac{J_{pm}}{J_p \cdot A_m^2}, \quad \varepsilon_p = \frac{J_p \cdot A_m^2 - J_{pm}}{A_p \cdot A_m \cdot J_m}, \quad J_0 = \frac{A_m \cdot J_m \cdot J_p}{J_p \cdot A_m^2 - J_{pm}}.$$

In the calculation of ε_m, ε_p and J_0 it was taken that $b_m = 3.55 \cdot 10^{-3}$ (Å^{-1}) (0.2 mm brass monodetector wall) and $b_p = 3.09 \cdot 10^{-3}$ (Å^{-1}) (4 mm aluminum PSD window). Figure 8 shows J_0, ε_p, ε_m as a function of the neutron wavelength. It is seen that there is little difference in the efficiency of the detectors and over the interval $1 \div 2$ Å the efficiency is $50 \div 70\%$. The dotted line is the calculated neutron count due to neutron absorption in a gas with the absorption coefficient $c_m = 0.7$ Å^{-1}. It demonstrates good agreement between the calculation and experiment.

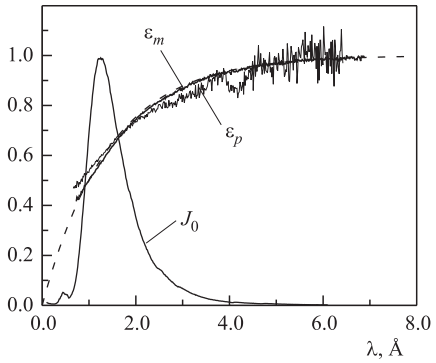

Fig. 8. The neutron detection efficiency of PSD (ε_p) and of the monodetector (ε_m), the dashed line is the calculated coefficient of neutron absorption by ^{3}He atoms in the monodetector, the curve J_0 is the calculated neutron flux density in front of the detector

For the registration of an intense neutron pulse at a pulsed reactor, of special importance is the operation speed of the detector. The parameter is assessed from the measured dependence of the count intensity on the neutron beam cross section that is set with a cadmium diaphragm. Figure 9 illustrates the dependence of the

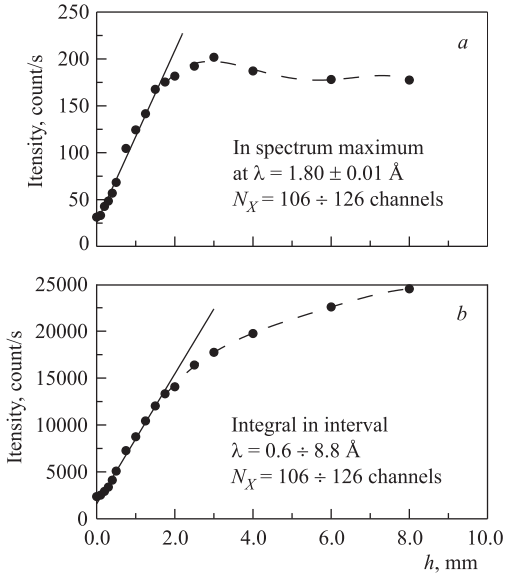

Fig. 9. The dependence of the neutron count on the height of the diaphragm on the detector (the width of the diaphragm is 1 mm): *a*) in the spectrum maximum if the wavelength is 1.8 Å and the registration is in one time channel; *b*) in the wavelength interval is 0.6 ÷ 8.8 Å

neutron count intensity on the height of the diaphragm (its width is 1 mm) for the cases of registration in one time channel (Fig. 9, *a*) and over the interval 0.6 ÷ 8.8 Å (Fig. 9, *b*). The data makes it possible to estimate that the maximum intensity for the height of the diaphragm 1.7 mm is $2.7 \cdot 10^5$ s^{-1} resulting in a dead time of the detector of 37 ns.

2.3.2. The Detector for the Small-Angle Mode. To perform small-angle scattering experiments with the spectrometer REMUR, a 32-counter detector is used. The detector consists of cylindrical counters of four sizes. Every eight equal size counters are arranged with a 45° spacing along a ring of some radius. The counters with the diameter 12, 18, 32 and 50 mm and the sensitive area length 50, 50, 95 and 110 mm are on the rings with the radius 75, 120, 190 and 300 mm, respectively. Further, the counters in two groups of 16 are positioned in two holders that are at an angle of 45° with respect to one

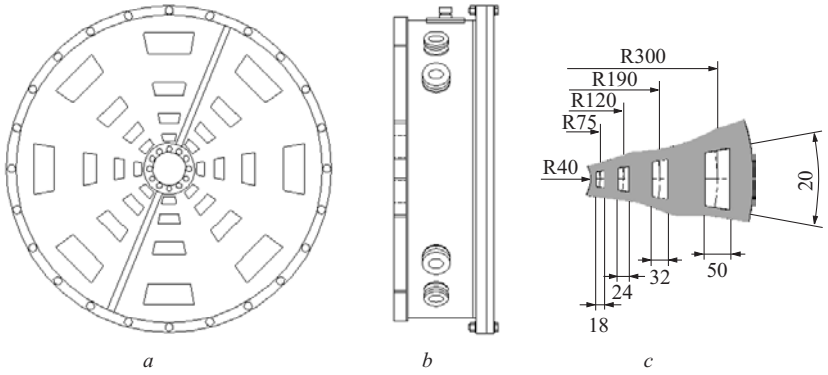

Fig. 10. The detector for the small-angle mode: *a*) front view; *b*) side view; *c*) counter windows

another and are 50 mm depth apart in the direction of the neutron beam. Figure 10 shows the front (*a*) and the side (*b*) view of the detector and the view of the windows (*c*) with their dimensions. The windows are made from sheet cadmium and determine the beam cross section on the counters.

Figure 11 shows the dependence of the background count intensity on the number of the time channel for the counters of the first ring (radius 150 mm) and of the fourth ring (diameter 600 mm). The presented data point to that the background count rate of the fourth ring counters is about 40 times higher than that of the first ring counters. This, as expected, is close to the ratio of the sensitive volumes of the fourth to first ring counters that equals 38.3. The detector can be installed at a distance of $1.5 \div 7.5$ m. As a result, for the neutron wavelength range $\lambda = 1.5 \div 10$ Å the detector covers the wave vector transfer interval $Q = 6 \cdot 10^{-3} \div 0.7$ Å^{-1}.

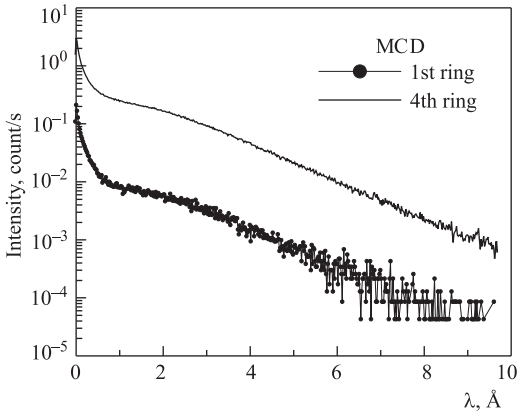

Fig. 11. The neutron background intensity for the counters of the 1st and 4th ring of the detector of the small-angle mode

2.4. The Sample Environment. The investigated sample is in the sample holder in the center of a goniometer. The goniometer has three axes of rotation with a rotation step of 0.01°, which enables:

1) rotation of the electromagnet by $\pm 90°$ around the neutron beam axis;

2) rotation of the sample together with the electromagnet by $\pm 20°$ around the vertical axis;

3) rotation of the electromagnet by $\pm 15°$ around the horizontal axis perpendicular to the neutron beam.

The goniometer can also be displaced manually in the direction along and perpendicular to the neutron beam within the limits ± 100 mm.

The magnetic field on the sample at room temperature is generated by the electromagnet with a set of replaceable polar shoes with the cross section 40×20 mm^2, 60×40 mm^2 or 110×70 mm^2. The magnetic field in the plane perpendicular to the beam can be chosen to have the direction from vertical to horizontal. The gap between the polar shoes can be set at $15 \div 70$ mm. The maximum magnetic field for the gap 15 mm between the 40×20 mm^2 cross-section polar shoes is 20 kOe and for the 110×70 mm^2 cross-section polar shoes it is 10 kOe.

For experiments at low temperatures a cryostat with 22 mm diameter quartz windows on the way of the neutron beam is used. The cryostat keeps the

temperature of the sample with a size of up to 40×40 mm^2 at $1.4 \div 600$ K with an accuracy of 0.01 K. The cryostat has a cryomagnet with a maximum strength of a vertically directed magnetic field of 30 kOe. The accuracy the magnetic field is set is ± 0.3 Oe in the interval $0 \div 3.4$ kOe and ± 30 Oe in the interval $3.4 \div 30$ kOe.

3. THE NEUTRON BEAM PARAMETERS

Figure 12, *a–c* depicts the wavelength dependence of the thermal neutron count and background count intensities (the neutron beam is shut off with a 1.5 mm cadmium sheet) for three polarization layouts: *a*) a straight polarizer for

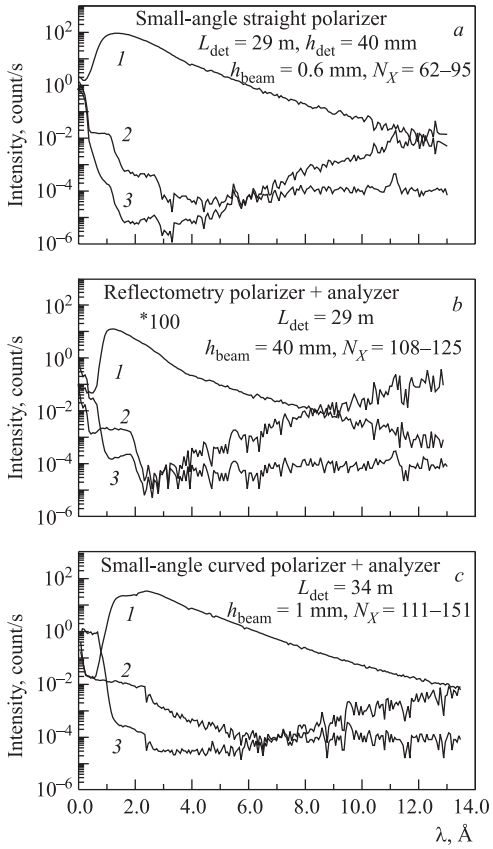

Fig. 12. The count intensities of thermal neutrons (curve *1*), of overcadmium neutrons (curve *2*) and of the ratio between them (curve *3*): *a*) — straight small-angle polarizer; *b*) — reflectometric polarizer with a 100 times intensity attenuator and a fan-like polarization analyzer; *c*) — curved polarizer with a fan-like polarization analyzer

Table 4. The neutron flux on the spectrometer REMUR

Equipment	$\Omega_{\rm pol}$, sterad	$\int_{\rm det}^{1.5{\rm MW}} N(\lambda)d\lambda$, n/(s·cm^2)	$\int_{\rm sample}^{2{\rm MW}} I(\lambda)d\lambda$, n/(s·cm^2)	$\frac{\int_{\rm sample}^{2{\rm MW}} I(\lambda)d\lambda}{\Omega}$, n/(s·cm^2)·sterad
1	2	3	4	5
Reflectometric polarizer + fan-like polarization analyzer	$2.0 \cdot 10^{-6}$	$3.6 \cdot 10^4$	$1.6 \cdot 10^5$	$8.0 \cdot 10^{10}$
Small-angle curved polarizer + fan-like polarization analyzer	$0.7 \cdot 10^{-6}$	$7.6 \cdot 10^3$	$6.8 \cdot 10^4$	$1.0 \cdot 10^{11}$
Small-angle straight polarizer	$1.7 \cdot 10^{-6}$	$1.5 \cdot 10^5$	$4.0 \cdot 10^5$	$2.4 \cdot 10^{11}$

the small-angle mode, a detector at 29 m from the moderator, the beam cross section 0.021 cm^2; *b*) a reflectometric polarizer with a fan-like analyzer, a detector at 29 m from the moderator, the beam cross section 1.4 cm^2; *c*) a curved polarizer with a fan-like analyzer, a detector at 34 m from the moderator, the beam cross section 0.035 cm^2. Using the obtained count intensity the neutron flux at sample position is calculated. The measured and calculated results are summarized in Table 4. It is taken into account that the integral efficiency of the detector is 70% and the transmission of the fan-like analyzer is 0.6. The second column in Table 4 shows the solid angle at which the exit of the polarizer is seen from the neutron detector. The third column presents the integral-over-wavelength neutron count rate of the detector at a nominal power of the reactor of 1.5 MW. The fourth column summarizes the calculated neutron flux at a sample position of 29 m from the moderator if the reactor power is 2 MW. The data in the latter column are important from the viewpoint of comparison with $2 \cdot 10^5$ n/s/cm^2, the value of an analogous parameter of the spectrometer SPN for the reactor power 2 MW. Finally, the fifth column presents the calculated polarized neutron flux density per solid angle which is interesting to compare with a maximum possible density of the unpolarized neutron flux of $7 \cdot 10^{11}$ n/(s $\cdot$ sm$^2\cdot$ sterad) in the water moderator and with $1.2 \cdot 10^{10}$ n/(s $\cdot$ cm$^2\cdot$ sterad), the value of the analogous parameter for the SPN spectrometer. It is seen that the neutron loss is minimum in the case of the straight small-angle polarizer and equals a factor of 0.7.

4. AUTOMATION OF THE SPECTROMETER PERFORMANCE

4.1. The System for Control of the Executive Mechanisms. The system controls the executive mechanisms of the small-angle spectrometer REMUR used as drives for step motors. The movement range of the executive mechanism is lim-

ited by end fixings and it has two reference points to monitor the most frequently used situations. The control system is constructed on the basis of the step-motor controller BCSM in VME standard and it has the following characteristics:

1) alternate control of 1–32 step-motors;

2) type of control: specified number of steps in the specified direction;

3) movement range is limited by two end fixings;

4) possibility of monitoring of up to two reference points over the entire movement range;

5) step frequency (starting from 1 Hz) is set by the program, it can be changed during the movement.

The control system employs the switcher-amplifiers of step-motors SMD-B2A as step-drive motors with the following characteristics:

1) alternate control of four motor;

2) number of motor windings — 2, 4;

3) switching pattern: unipolar and bipolar;

4) current in the motor winding — 2/4 A;

5) switcher multiplexes the end fixings and reference points of the selected executive mechanism;

6) switcher is made in CAMAC standard.

The control block of the physical setup BCFU enables the monitoring of the state of the gate and of the phase of the neutron beam chopper.

The panel for manual control executes control of the executive mechanisms right at their working site and performs:

1) selection of the number $N = 1 \div 32$ of the executive mechanisms;

2) indication of end fixings and reference points;

3) setting of the frequency of the control signal of the step motors within the limits 1 Hz $\div$ 1 kHz.

The step motors are fed by the power supply PSU 32/10A.

The test block of the control system performs the following auxiliary functions:

- start-, monitor-, and gate-signal formation,
- indication of start switching, neutron count by the monitor and of the gate state,
- gate-signal filtration,
- multiplication of such signals,
- test mode of signal formation.

The system for control of the executive mechanisms of the spectrometer includes:

1) diaphragms 1, 2, 3,

2) platforms 1, 2, 3,

3) neutron polarizers,

4) cadmium shutter,

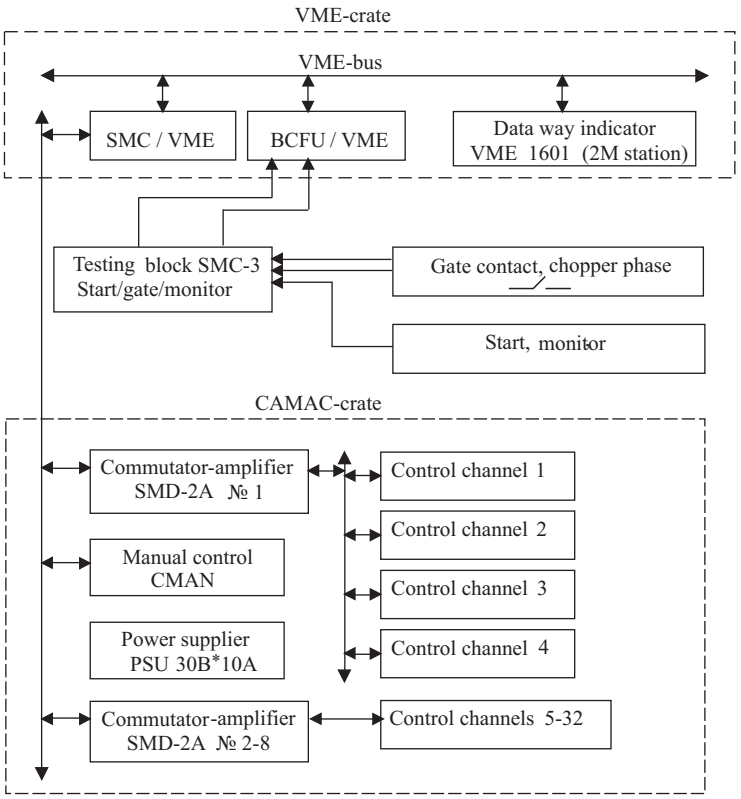

Fig. 13. The structural scheme of the control system of the REMUR executive mechanisms

5) goniometer,

6) polarization analyzer, etc.

Figure 13 presents the block scheme of the control system of the executive mechanisms of the spectrometer REMUR.

4.2. The Data Acquisition System. The equipment for experimental data acquisition from the detectors PSD and MCD, power supply and the detector control are executed as CAMAC and VME crates (Fig. 1).

The PSD measuring and data acquisition structure includes 256 position and 2048 time channels [15]. The duration of the time channel is 128 μs.

A separate measuring channel for MCD has the following characteristics: the number of time channels is 2048, the time channel width is 64 μs, the word length is 24 bits. Signals from an individual MCD counter, via an amplifier and the CNE detector number coder in a CAMAC crate, comes right to the DSP

processor input of the VME crate where they are processed and then recorded in the histogram memory block HM-32. As the measuring cycle completes the data are read from the histogram memory and are transmitted to a PC for further viewing and processing.

To enable the acquisition and initial viewing of the spectra obtained in the experiment, a SONIX packet-based software complex is used. The software complex includes the programs TOFA and VSP responsible for the operation of the data acquisition and control system of the spectrometer. Acquisition, processing and transmission to the histogram memory NM-32 of the spectrometric data are performed by a soft hardware complex on the basis of the processor DSP in VME standard. The main function of the program TOFA is to specify the parameters and the experimental data acquisition time with their further transmission to the hard disk of the VME system. VSP is a service program that enables express-visualization of the obtained data by reading directly from the histogram memory. Also, the program has a number of other possibilities that allow data assessment in the course of measurements. The primary procession of the obtained experimental data is done with a program written in the language OPEN-G2. The program allows the presentation of the detector count as a function of the time channel number n_t, counter number n_c, wavelength and of the wave number transfer: $I(n_t,\ n_c)$, $I(\lambda)$, $I(Q)$. The program adds up the counts of detectors situated on one of the four rings; subtracts background counts; normalizes to some specified count, e.g., from a standard scatterer; calculates the macroscopic scattering cross sections $\sum^{+}(q)$ and $\sum^{-}(q)$ for «+» and «-» spin states when the data on polarized neutron beam scattering are used.

4.3. The Spectrometer Software. The experiment control software is based on the Sonix complex [24] completed with some spectrometer-specific programs. The Sonix complex includes modules for control of data acquisition and spectra recording, for control of beam intensity and the other experimental conditions, such as the existence and frequency of reactor start signals, phasing of the chopper, opening of the beam gate, etc., for control of the movable components of the spectrometer and of the thermoregulator EUROTERM. Specifically for the spectrometer there were developed and introduced into the scheme:

- module for control of current sources,
- module for rearranging of physical axes,
- program for express-visualization of the experimental data,
- program for adjustment.

To rearrange physical axes as specified in an individual experiment, a special module which calculates the adjusting platform displacement from the given glancing angle or the coordinate of the target (sample position) is used.

The express-visualization program can be used for the experimental data quality assessment. The program makes it possible to vary the scale of the axes (without specification, the scale is set automatically), choose the neutron

count viewing type (three-dimensional surface, level lines, color map), rotate the three-dimensional graph, specify the region of summation, store the picture in the format JPG and send it to print. The maximum number of neutron count spectra shown at the same time is four.

The purpose of experimental determination of an optimal state of the setup there serves the adjustment program [25]. It provides for the possibility of control of the equipment and of the measuring process, effective access to the stored data, express spectra processing, spectra viewing as well as some service functions.

To control the experiment in the automatic mode a specification (script) is written in a special language. For the purpose of simplifying the procedure a script editor adapted to the spectrometer has been developed. The user who works on a personal computer fills in, one after another, the areas on the pages of the form and finally gives a command to form a specification file. The possibility of automatic forwarding of a ready program to a VME-computer and loading of a ready script for viewing and editing is also envisaged.

The general-purpose program **OpenG2** [26, 27] for viewing and express analysis of the spectra measured with the IBR-2 spectrometers is completed with the module **openg2_spn2** that realizes special-purpose functions making it possible to work with the data measured with the spectrometer REMUR in the small-angle or reflectometric modes. The user interface of the program for small-angle data allows fast selection between various functions and versions of data grouping, including the selection of any group of 32-point scattering detectors arranged, e.g., on one radius or ring by a simple mouse click. On user's request, workspaces are formed of the processed spectra for the purpose of further interactive procession employing the standard functions of the program **OpenG2** or storing them in files.

The Sonix complex is mainly realized on a VME-computer in the operation system OS-9. The setup adjustment and express viewing programs are in MS Windows, and the program for preliminary data procession is in Solaris on a SUN workstation.

5. THE NEUTRON REFLECTIVITY MEASURING TECHNIQUE

5.1. Magnetically Noncollinear Structures. If the magnetization vector in the investigated sample is noncollinear with the magnetic field strength vector on the sample, the neutron reflection coefficient is a 2×2 matrix whose elements R^{ij} are the neutron reflection coefficients from initial i to final j neutron spin state. In accordance with the preceding notation the states i and j are the states «+» or «-». The neutron count intensity of the detector can be written as:

$$I^{\nu\varphi} = I_0 \frac{1}{2} \begin{pmatrix} 1+P_a & 0 \\ 0 & 1-P_a \end{pmatrix} \begin{pmatrix} 1-f_2 & f_2 \\ f_2 & 1-f_2 \end{pmatrix} \begin{pmatrix} R^{++} & R^{-+} \\ R^{+-} & R^{--} \end{pmatrix} \times$$
$$\times \begin{pmatrix} 1-f_1 & f_1 \\ f_1 & 1-f_1 \end{pmatrix} \frac{1}{2} \begin{pmatrix} 1+P_p & 0 \\ 0 & 1-P_p \end{pmatrix} \begin{pmatrix} 1 \\ 1 \end{pmatrix}, \quad (3)$$

where $I_0 = \frac{1}{2} I'_0 t_a t_p \varepsilon$, I'_0 is the inlet neutron beam intensity in the polarizer, ε is the detector efficiency, $t_p = (t_p^+ + t_p^-)/2$, $t_a = (t_p^+ + t_p^-)/2$, $P_p = (t_p^+/t_p^- - 1)/(t_p^+/t_p^- + 1)$, $P_a = (t_a^+/t_a^- - 1)/(t_a^+/t_a^- + 1)$, t_p^+, t_p^- and t_a^+, t_a^- are the transmission coefficients of the polarizer and the analyzer, respectively; f_1 and f_2 are the spin-flip probability in the first and the second spin-flipper, respectively; ν and φ stand for the states «on» or «off» of the first and the second spin-flipper, respectively. Introducing the notation $F_1 = 2f_1 - 1$ and $F_2 = 2f_2 - 1$ we rewrite Eq. (3) for the matrix element $I^{\nu\varphi}$:

$$I^{\text{off,off}} = I_0[R^{++}(1+P_p)(1+P_a) + R^{--}(1-P_p)(1-P_a) +$$
$$+ R^{+-}(1+P_p)(1-P_a) + R^{-+}(1-P_p)(1+P_a)]/4,$$

$$I^{\text{on,on}} = I_0[R^{++}(1-F_1P_p)(1-F_2P_a) + R^{--}(1+F_1P_p)(1+F_2P_a) +$$
$$+ R^{+-}(1-F_1P_p)(1+F_2P_a) + R^{-+}(1+F_1P_p)(1-F_2P_a)]/4,$$

$$I^{\text{off,on}} = I_0[R^{++}(1+P_p)(1-F_2P_a) + R^{--}(1-P_p)(1+F_2P_a) +$$
$$+ R^{+-}(1+P_p)(1+F_2P_a) + R^{-+}(1-P_p)(1-F_2P_a)]/4,$$

$$I^{\text{on,off}} = I_0[R^{++}(1-F_1P_p)(1+P_a) + R^{--}(1+F_1P_p)(1-P_a) +$$
$$+ R^{+-}(1-F_1P_p)(1-P_a) + R^{-+}(1+F_1P_p)(1+P_a)]/4. \quad (4)$$

From the system of Eqs. (4) we determine the neutron reflectivities:

$$R^{++} = \frac{1}{4I_0 f_1 f_2 P_p P_a}[I^{\text{off,off}}(F_1P_p+1)(F_2P_a+1) + I^{\text{on,on}}(P_p-1)(P_a-1) +$$
$$+ I^{\text{off,on}}(F_1P_p+1)(P_a-1) + I^{\text{on,off}}(P_p-1)(F_2P_a+1)],$$

$$R^{--} = \frac{1}{4I_0 f_1 f_2 P_p P_a}[I^{\text{off,off}}(F_1P_p-1)(F_2P_a-1) + I^{\text{on,on}}(P_p+1)(P_a+1) +$$
$$+ I^{\text{off,on}}(F_1P_p-1)(P_a+1) + I^{\text{on,off}}(P_p+1)(F_2P_a-1)],$$

$$R^{+-} = \frac{1}{4I_0 f_1 f_2 P_p P_a}[I^{\mathrm{off,off}}(F_1P_p+1)(F_2P_a-1) + I^{\mathrm{on,on}}(P_p-1)(P_a+1)+ \\ + I^{\mathrm{off,on}}(F_1P_p+1)(P_a+1) + I^{\mathrm{on,off}}(P_p-1)(F_2P_a-1)],$$

$$R^{-+} = \frac{1}{4I_0 f_1 f_2 P_p P_a}[I^{\mathrm{off,off}}(F_1P_p-1)(F_2P_a+1) + I^{\mathrm{on,on}}(P_p+1)(P_a-1)+ \\ + I^{\mathrm{off,on}}(F_1P_p-1)(P_a-1) + I^{\mathrm{on,off}}(P_p+1)(F_2P_a+1)]. \quad (5)$$

From Eq. (5) it is seen that in addition to the count intensities $I^{\mathrm{off,off}}$, $I^{\mathrm{off,on}}$, $I^{\mathrm{on,off}}$, $I^{\mathrm{on,on}}$ one must know the parameters I_0, f_1, f_2, P_p, P_a that characterize the spectrometer itself. The determination of the parameters of the spectrometer (calibration of the spectrometer) is done using the method 3P2S (3 polarizers and 2 spin-flippers) [28–30] that consists in that the count intensity is measured four times without a sample, $I_e^{\mathrm{off,off}}$, $I_e^{\mathrm{off,on}}$, $I_e^{\mathrm{on,off}}$ and $I_e^{\mathrm{on,on}}$, and four measurements with a sample-calibrator, $I_c^{\mathrm{off,off}}$, $I_c^{\mathrm{off,on}}$, $I_c^{\mathrm{on,off}}$ and $I_c^{\mathrm{on,on}}$. The measurements without a sample effectively correspond to the case $R^{++} = R^{--} = 1$ and $R^{+-} = R^{-+} = 0$. The measurements allow the determination of the parameters I_0, f_1, f_2 and P_p, P_a:

$$I_0 = \frac{2(I_e^{\mathrm{off,off}} I_e^{\mathrm{on,on}} - I_e^{\mathrm{off,on}} I_e^{\mathrm{on,off}})}{I_e^{\mathrm{off,off}} + I_e^{\mathrm{on,on}} - I_e^{\mathrm{off,on}} - I_e^{\mathrm{on,off}}},$$
$$P_p P_a = \frac{(I_e^{\mathrm{off,off}} - I_e^{\mathrm{off,on}})(I_e^{\mathrm{off,off}} - I_e^{\mathrm{on,off}})}{I_e^{\mathrm{off,off}} I_e^{\mathrm{on,on}} - I_e^{\mathrm{off,on}} I_e^{\mathrm{on,off}}}, \quad (6)$$
$$f_1 = \frac{1}{2}\left(1 + \frac{I_e^{\mathrm{on,on}} - I_e^{\mathrm{on,off}}}{I_e^{\mathrm{off,off}} - I_e^{\mathrm{off,on}}}\right), \quad f_2 = \frac{1}{2}\left(1 + \frac{I_e^{\mathrm{on,on}} - I_e^{\mathrm{off,on}}}{I_e^{\mathrm{off,off}} - I_e^{\mathrm{on,off}}}\right).$$

A sample for which there hold the relationships $R_c^{+-} = R_c^{-+} = 0$ and $R_c^{++} \neq R_c^{--}$ is taken as a sample-calibrator. In the measurements with a calibrator there are separately determined the parameters P_p and P_a and the reflection coefficients of the calibrator R_c^{++} and R_c^{--}:

$$P_p = \sqrt{\frac{C_1 C_2}{C_3 C_4}}, \quad P_a = \sqrt{\frac{C_1 C_4}{C_3 C_2}},$$
$$R_c^{++} = C_5\left\{1 + \sqrt{\frac{C_2 C_4}{C_3 C_1}}\right\}, \quad R_c^{--} = C_5\left\{1 - \sqrt{\frac{C_2 C_4}{C_3 C_1}}\right\}, \quad (7)$$

where $C_1 = I_c^{\mathrm{off,off}} + I_c^{\mathrm{on,on}} - I_c^{\mathrm{off,on}} - I_c^{\mathrm{on,off}}$, $C_2 = F_2(I_c^{\mathrm{off,off}} - I_c^{\mathrm{on,off}}) - I_c^{\mathrm{on,on}} + I_c^{\mathrm{off,on}}$, $C_3 = F_1F_2 I_c^{\mathrm{off,off}} + I_c^{\mathrm{on,on}} + F_1 I_c^{\mathrm{off,on}} + F_2 I_c^{\mathrm{on,off}}$, $C_4 = F_1(I_c^{\mathrm{off,off}} - I_c^{\mathrm{off,on}}) - I_c^{\mathrm{on,on}} + I_c^{\mathrm{on,off}}$, $C_5 = \dfrac{C_3}{2I_0 f_1 f_2}$.

5.2. Magnetically Collinear Structures. If neutrons are reflected from a magnetically collinear structure they do not experience a transition from one spin state to the other. So, different from zero are only the reflection coefficients $R^{++} = R^{+}$ and $R^{--} = R^{-}$, where R^{+} and R^{-} are the reflection coefficients of neutrons with the initial spin state «+» or «-», respectively.

To determine R^{+} and R^{-}, it suffices to use an experimental layout with one spin-flipper without polarization analyzers. Then the count intensity is measured without a sample, I_e, and with a sample with the spin-flipper on, I^{on}, and off, I^{off}:

$$\begin{aligned} R^{+} &= \frac{[1 - P_p(1 - 2f_1)]I^{\mathrm{off}} - (1 - P_p)I^{\mathrm{on}}}{2f_1 P_p I_e}, \\ R^{-} &= \frac{(1 + P_p)I^{\mathrm{on}} - [1 + P_p(1 - 2f_1)]I^{\mathrm{off}}}{2f_1 P_p I_e}. \end{aligned} \tag{8}$$

From Eq. (8) it is seen that it is also necessary to know the parameters of the spectrometer f_1 and P_p. The parameters f_1 and P_p can be determined by employing the experimental layout with two spin-flippers and a polarization analyzer described in the previous section. However, if one uses a calibrator with a known reflection coefficient, the parameters f_1 and P_p can be determined from the experiment with one spin-flipper without a polarization analyzer:

$$f_1 = \frac{I^{\mathrm{off}} - I^{\mathrm{on}}}{2I^{\mathrm{off}} - I_e(R_c^{++} + R_c^{--})}, \quad P_p = \frac{2I^{\mathrm{off}} - I_e(R_c^{++} + R_c^{--})}{I_e(R_c^{++} - R_c^{--})}. \tag{9}$$

6. EXPERIMENTS EMPLOYING PSD

6.1. Software Support of the Experiment. To run the experiment and control the experimental data acquisition, the program **NEU00.exe** installed on a PC is used. The stored PSD data are written as a spectral file in the binary form. The program **NEU00.exe** executes the control subregimes **Check Start** and **Main Start**. The **Check Start** is used for neutron measurements of short duration carried out for the purpose of spectrometer tuning. The experimentalist then specifies the acquisition time of one spectrum in hours, minutes and seconds. In the process of spectrum the acquisition time is recalculated in terms of the number of pulses (starts) by the formula $m(\mathrm{starts}) = 4.8163 \cdot t\,(\mathrm{s})$. The file name is of the type **spectABN**. The file name must not have more than 8 symbols. The name of the spectrum **spect** is specified by the user and may contain from 1 to 5 symbols. Further, in the course of measurements the indices **ABN** are automatically added to the file name. The indices **A** and **B** correspond to the state of the first and the

second spin-flipper, respectively, and the number **N** stands for the file number. The letter «P» stands for the spin-flipper state «off» and the letter «M» stands for the spin-flipper state «on». The subregime **Main Start** provides for automatic switching of the spin-flipper and enables data acquisition for each state of a pair of spin-flippers during a period of time specified for the given state. The different states of the spin-flipper alternate and repeat in cycles. This excludes the effect of changes in the neutron beam intensity with time. Varying the ratio between acquisition times for the different states it is possible to optimize the measurement and carry it out in a shorter time. On completion of every measuring cycle spectra are recorded as files forming, with time, a progressive sum. As the specified time expires, to the existing files there are added files with the same name but a higher file number. This ensures safety of the data acquired during a measuring time preceding any failure in spectrum acquisition. The program **Main Start** envisages four measuring regimes in which the following spectra are created:

• **regime 1** (spin-flippers off) — spectPPN

• **regime 2** (first spin-flipper on) — spectPPN, spectMPN

• **regime 3** (second spin-flipper on) — spectPPN, spectPMN

• **regime 4** (two spin-flippers on) — spectPPN, spectMPN, spectPMN, spectMMN.

6.2. Experimental Data Preprocessing. By means of the program **NEUTXT.exe** the spectrum binary file **spectABN** is changed into the text file **spectABN.txt** of the form:

• First line presents the numbers 256 (the number of PSD coordinate channels PSD) and 2048 (the number of PSD time channels).

• Second line presents the number of reactor starts and the integral neutron count over all channels.

• Starting from the third line there is presented the two-dimensional matrix 2048 (number of lines) $\times$ 256 (number of columns) of neutron count per time channel per coordinate channel.

For preprocessing of the data a packet of programs in the language FORTRAN has been created. The input files for the programs are the text files of spectra **spectABN.txt** and the output is the data text files **file.dat** containing columns of figures. The files **file.dat** are ready for use in standard graphics editing programs GRAPHER or ORIGIN or for further processing.

The following *data preprocessing programs* exist:

1. *neu00.exe* — viewing of the two-dimensional distributions $J(N_\lambda, N_x)$ and of the one-dimensional distributions $J(N_\lambda)$ and $J(N_x)$;

2. *lam_as.for* — calculation of the dependence of the neutron count intensity on the neutron wavelength for a specified interval ΔN_x;

3. *x_as.for* — determination of the spatial distribution of the neutron count intensity for a specified interval ΔN_λ;

4. *f1_f2_pa.for* — determination of the spin-flip probability in the first and in the second spin-flipper and of the product of the polarization efficiency of the polarizer by that of the analyzer from the data on the count intensity obtained with the experimental layout «polarizer → first-spin-flipper → second spin-flipper → analyzer»;

5. *pa_r.for* — determination of the spin-flip probabilities in the spin-flippers and of the polarization efficiency of the polarizer and of the analyzer from the data on the count intensity obtained with the experimental layout «polarizer → first spin-flipper → second spin-flipper → analyzer» and «polarizer → first spin-flipper → calibrator → second spin-flipper → analyzer»;

6. *p.for* — determination of the product $P_p\ P_a$ in the experiment with one spin-flipper and polarization analyzer; the spin-flip probability by one spin-flipper is unity;

7. *drt_as.for* — determination of the reflection coefficient from four count intensities; the polarization efficiency of the polarizer and of the analyzer, the spin-flip probabilities in the two spin-flippers and the count intensity I_0 are also introduced.

6.3. Model Calculations. The final goal of the reflectometric experiment is obtaining of the experimental data for the determination of the neutron reflection coefficient $R_{\rm exp}$, actual parameters of the structure (nuclear and magnetic optic potentials in individual layers of the structure, thickness of the layers, interface roughness, etc.). Since the angular and the time resolution of the spectrometer is finite the experimental reflection coefficient is a convolution of the actual neutron reflection coefficient $R(q)$ and the spectrometer resolution functionp $f(\theta, t)$:

$$R_{\rm exp} = \int j_0(\theta,\lambda)\ f(\theta,t)\ R(q)\ d\theta\ dt \Big/ \int j_0(\theta,\lambda)\ f(\theta,t)\ d\theta\ dt, \qquad (10)$$

where $j_0(\theta,\lambda)$ is the neutron flux density at the exit of the neutron polarizer, θ is the neutron glancing angle on the investigated sample. To change Eq. (10) into a simpler equation, let us note that, the transferred wave number q is related with θ and the wavelength λ as $q = 4\pi\ \sin(\theta)/\lambda$. Then, the moderator-to-detector neutron flight time t is related with λ as $t\ ({\rm ms}) = 3.956\lambda({\rm \AA})L(m)$, where L is the moderator-to-detector distance. Taking advantage of the relationships it is possible, step by step, to pass from the variable t to λ and further from the variables λ and θ to the variable q. Next, knowing the average wavelength $\lambda_{\rm av}$ with the mean square accuracy $\delta\lambda \ll \lambda_{\rm av}$ and the glancing angle $\theta_{\rm av}$ with the mean square accuracy $\delta\theta < \theta_{\rm av}$ we can rewrite Eq. (10) as:

$$R_{\rm exp}(q_{\rm av}) = \int j_0(q,q_{\rm av})\ f(q,q_{\rm av})\ R(q)\ dq \Big/ \int j_0(q,q_{\rm av})\ f(q,q_{\rm av})\ dq, \quad (11)$$

where $q_{\rm av} = 4\pi\ \sin(\theta_{\rm av})/\lambda_{\rm av}$. The integration over q is carried out within the limits of variation of the wave number from $q_{\rm min} = 4\pi\ \sin(\theta_{\rm av} - \Delta\theta/2)/(\lambda_{\rm av} +$

$\Delta\lambda/2)$ to $q_{\max} = 4\pi \sin(\theta_{\rm av} + \Delta\theta/2)/(\lambda_{\rm av} - \Delta\lambda/2)$, and $\Delta\theta$ and $\Delta\lambda$ are the intervals of the glancing angle and neutron wavelength, respectively. Since q varies little around $q_{\rm av}$ the resolution function can be presented in the form of a Gauss function as $f(q, q_{\rm av}) = c \exp(-(q - q_{\rm av})^2/2\sigma_q^2)$, where $c = 1/2\pi\sigma_q^2$, $\sigma_q = q[(\delta\theta/\theta_{\rm av})^2 + (\delta\lambda/\delta\lambda_{\rm av})^2]^{1/2}$, $\delta\theta$ and $\delta\lambda$ are calculated. To calculate $\delta\theta$, we have:

$$\delta\theta = [(h_1^2 + h_2^2/3)]^{1/2}/L_{\rm dia}, \tag{12}$$

where h_1 and h_2 are the half width of the first and the second diaphragm and $L_{\rm dia}$ is the distance between the diaphragms. The first is the diaphragm at the exit of the polarizer. The role of the second diaphragm there can play either the diaphragm with the half width $h_{\rm fs}$ in front of the sample or the diaphragm with the half width $h_{\rm s}$ on the sample or the diaphragm with the half width $h_{\rm det}$ on the detector (several PSD position channels can play the role of the latter). To choose h_2 and $L_{\rm dia}$, there are used the parameters of the diaphragm for which the ratio between its half width and the distance to the first diaphragm is smallest. Then $h_2 = h_{\rm fs}$ and $L_{\rm dia} = L_{\rm fs}$ if $h_{\rm fs}/L_{\rm fs}$ is smallest, $h_2 = h_{\rm s}$ and $L_{\rm dia} = L_{\rm s}$ if $h_{\rm s}/L_{\rm s}$ is smallest and finally $h_2 = h_{\rm det}$ and $L_{\rm dia} = L_{\rm det}$ if $h_{\rm det}/L_{\rm det}$ is smallest. It should be noted that if $l_{\rm s} \sin(\theta) < h_{\rm s}$ or if there is no diaphragm on the sample, the sample itself plays the role of that diaphragm and $h_{\rm s} = l_{\rm s} \sin(\theta)/2$, where $l_{\rm s}$ is the length of the sample along the beam.

For the mean square wavelength $\delta\lambda$ we have

$$\delta\lambda = 3.956 \{[(\tau/2)^2 + (\Delta t/2)^2]/3\}^{1/2}/L, \tag{13}$$

where $\tau = 0.320$ ms is the thermal neutron pulse duration, Δt is the width of the time channel of the detector which is equal to 0.128 ms for PSD and to 0.064 ms for MCD. For $L = 34$ m and $\Delta t = 0,128$ ms we obtain that the wavelength resolution of the spectrometer is $\delta\lambda = 0.011$ Å if PSD is used.

CONCLUSION

The effort to construct the new polarized neutron spectrometer was based on many-year experience of investigations of the magnetic structure of bulk magnetic and superconducting materials [31–33] and of multiplayer magnetically non-collinear nanostructures [34]. The orientation towards the creation of wide-band and wide-aperture polarization instruments in combination with position-sensitive detection together with the adopted concept of investigations with reflectometry and small-angle scattering as complimentary methods appears quite justified in the case of a spectrometer at a pulsed neutron source. Figure 14 shows the wavelength dependence of the gain factor for the parameter $P^2 I$ in the new spectrometer REMUR in comparison with the SPN spectrometer. It is seen that the

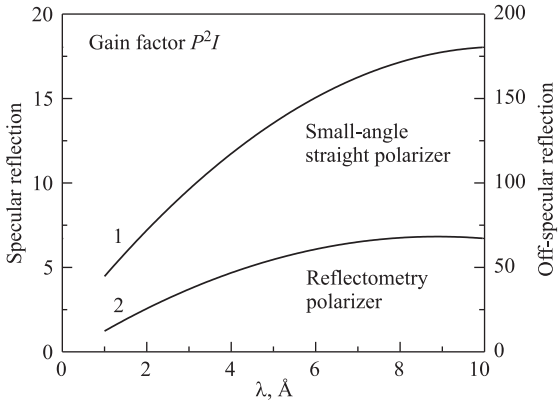

Fig. 14. The gain factor of the parameter P^2I in the small-angle spectrometer REMUR with small-angle and reflectometric polarizers in comparison with the SPN spectrometer for the cases of specular and diffuse isotropic neutron scattering

spectrometer efficiency has grown tens of times in the case of specular reflection and hundreds of times in the case of diffuse scattering measurements.

Making an organic whole the measuring scheme of the spectrometer was completed with our newly developed methods, including spatial splitting of the neutron beam [35, 36] and generation of standing or enhanced standing neutron waves in a layered structure [37, 38].

With the new spectrometer a first investigation of the coexistence of superconductivity and magnetism in a bilayer and in the periodic structure Fe/V [39] has been performed confirming the REMUR operation efficiency.

In conclusion we want to thank A. I. Okorokov, S. V. Grigoriev, V. A. Ul'yanov, V. M. Pusenkov and A. F. Schebetov from PNPI who took active part in the creation of polarization instruments, A. Sirotin, A. Kirilov, A. Bogdzel, A. F. Levchanovskii and V. Zhuravlev from the FLNP Scientific Experimental Division of IBR-2 Spectrometric Complex who effectively participated in the creation of automation and control, neutron detection, data acquisition and processing systems, V. I. Konstantinov, A. A. Kustov and N. A. Volkov from FLNP Design Bureau who developed mechanical blocks, and all the others who contributed to the creation and startup of the spectrometer.

The authors thank T. F. Drozdova for the English translation of this paper.

REFERENCES

1. *Drabkin G. M. et al.* // ZhETF. 1969. V. 29. P. 261.
2. *Rekveldt M. Th.* // J. de Physique. 1971. V. 32. P. 579.

3. *Aksenov V. L., Nikitenko Yu. V.* // Surface. X-Ray Synchrotron and Neutron Investigations. 1997. V. 12. P. 5;
Aksenov V. L., Nikitenko Yu. V. // Surface Investigation. 1998. V. 13. P. 1461.
4. *Okorokov A. I. et al.* // J. de Physique. 1982. V. 43. P. 97.
5. *Deriglazov V. V. et al.* // Proc. of PNCMI-96. June 18–20, Dubna. 1996.
6. *Mezei F.* // Z. Phys. 1972. V. 255. P. 146.
7. *Felcher G. P.* // Physica B. 1999. V. 267–268. P. 154.
8. *Korneev D. A.* // Nucl. Istr. Meth. 1980. V. 169. P. 65.
9. *Korneev D. A., Kudrjashev V. A.* // Nucl. Instr. Meth. 1981. V. 179. P. 509.
10. *Korneev D. A. et al.* // Proc. of the 2nd Intern. Conf. on Surface X-Ray and Neutron Scattering, Bad Honnef, June 25–28, 1991.
11. *Kortright J. B. et al.* // JMMM. 1999. V. 207. P. 7.
12. *Moon R. B., Riste T., Koehler W. C.* // Phys. Rev. B. 1969. V. 181. P. 920.
13. *Shabalin E. P.* Fast Pulsed Neutron Reactors. M.: Atomizdat, 1976.
14. *Ul'yanov V. A. et al.* Focused Analyzer of Neutron Polarization (in preparation).
15. *Fateev O. V. et al.* // PTE. 2001. V. 2. P. 5;
Fateev O. V. et al. // Instrum. and Exp. Tech. 2001. V. 44. P. 137.
16. *Mezei F.* // Commun. Phys. 1976. V. 1. P. 81.
17. *Maier-Leibnitz H., Springer T.* // Reactor Sci. Technol. 1963. V. 17. P. 217.
18. *Mikhailova V. E. et al.* Preprint LINP-696, 1981.
19. *Dokukin E. B., Nikitenko Yu. V.* // Nucl. Instr. Meth. A. 1993. V. 330. P. 462.
20. *Grigoriev S. V.* Preprint PINP-1840, 1992.
21. *Grigoriev S. V., Okorokov A. I., Runov V. V.* // Nucl. Instr. Meth. A. 1997. V. 384. P. 451.
22. *Grigoriev S. V. et al.* RF Gradient Spin-Flippers on the Polarized Neutron Spectrometer REMUR (in preparation).
23. *Abov Yu. G., Gul'ko A. D., Krupchitskii P. A.* Polarized Slow Neutrons. M.: Atomizdat, 1966.
24. *Kirilov A. S.* Current State and Perspectives of IBR-2 Instrument Control Software // Proc. of the Second Intern. Workshop on Data Acquisition Systems for Neutron Experimental Facilities (DANEF-2000). JINR E10-2001-11. Dubna, 2001.
25. *Yudin V. E.* MS Windows Programs for Adjusting the REMUR Spectrometer. JINR Preprint, P13-2003-12. Dubna, 2003.
26. *Litvinenko E. I.* The Implementation of NeXus Data Format in OpenG2 Software Package // Proc. of the Second Intern. Workshop on Data Acquisition Systems for Neutron Experimental Facilities (DANEF-2000). JINR E10-2001-11. Dubna, 2001.
27. *Kirilov A. S. et al.* Development of the Sonix Complex for the Spectrometer YuMO at the IBR-2 Reactor. JINR Commun., P13-2003-66. Dubna, 2003.
28. *Por P. T., Kraan W. H., Rekveldt M. Th.* // Nucl. Instr. Meth. A. 1994. V. 339. P. 550.
29. *Majkrzak C. F.* // Physica B. 1996. V. 221. P. 342.
30. *Fredrikze H., van de Kruijs R. W. E.* // Physica B. 2001. V. 297. P. 143.
31. *Aksenov V. L. et al.* // Physica B. 1995. V. 213–214. P. 134.
32. *Aksenov V. L., Dokukin E. B., Nikitenko Yu. V.* // Physica B. 1995. V. 213–214. P. 100.

33. *Aksenov V. L. et al.* // Pis'ma ZhETF. 1995. V. 61. P. 294.
34. *Aksenov V. L. et al.* // Physica B. 2003. V. 335. P. 147.
35. *Aksenov V. L., Nikitenko Yu. V., Kozhevnikov S. V.* // Physica B. 2001. V. 297. P. 94.
36. *Kozhevnikov S. V.* Investigation and Application of the Neutron Beam Spatial Splitting Effect in Magnetic Media. Candidate of Science (Phys&Math) Thesis. 14-02-115, Dubna, 2002.
37. *Aksenov V. L., Nikitenko Yu. V.* // Physica B. 1999. V. 267–268. P. 313.
38. *Aksenov V. L., Nikitenko Yu. V.* // Physica B. 2001. V. 297. P. 101.
39. *Aksenov V. L. et al.* // JINR NEWS. 2003. V. 4. P. 25.

Received on May 27, 2004.

Корректор *Т. Е. Попеко*

Подписано в печать 06.07.2004.
Формат 60 × 90/16. Бумага офсетная. Печать офсетная.
Усл. печ. л. 2,18. Уч.-изд. л. 3,11. Тираж 170 экз. Заказ № 54512.

Издательский отдел Объединенного института ядерных исследований
141980, г. Дубна, Московская обл., ул. Жолио-Кюри, 6.
E-mail: publish@pds.jinr.ru
www.jinr.ru/publish/